RSC Advances

PAPER

View Article Online
View Journal | View Issue

Cite this: *RSC Adv.*, 2015, **5**, 67267

Biocomposite adhesion without added resin: understanding the chemistry of the direct conversion of wood into adhesives†

Jeffrey A. Dolan,[a] Noppadon Sathitsuksanoh,[b] Katia Rodriguez,[c] Blake A. Simmons,[bd] Charles E. Frazier[ac] and Scott Renneckar*[e]

Received 22nd May 2015
Accepted 30th July 2015

DOI: 10.1039/c5ra09676f

www.rsc.org/advances

In this work we revealed how the controlled degradation of wood surfaces with infrared light from a CO_2 pulsed laser facilitated adhesion between two biobased substrates without the use of additional resins. Laser modification physically and chemically altered the natural biopolymer organization of lignocellulosic materials enabling adhesion when subsequently hot pressed using typical industrial equipment. Surface analysis of the modified material revealed that laser modification changed the native wood morphology as it appeared to coalesce, while the hemicelluloses were depolymerized and vaporized, and the surface was enriched with cellulose II and lignin. The latter two materials made up over 90% of the solid surface. The lignin itself was partially depolymerized resulting in enrichment of cinnamyl alcohol end groups, which are structures arising from homolytic cleavage of the β-O-4 linkages. An adhesion mechanism related to heat induced coupling in the presence of structural polysaccharides was discussed. Laser modification of wood followed by hot pressing provided a bio-based alternative for petroleum and natural gas derived wood adhesives and provides a path towards utilizing cellulose and lignin directly as structural adhesives.

Introduction

Wood is a ubiquitous natural resource that is a cornerstone material for industrialized society. It has been cited as a sustainable resource for biofuels, has been used for more than a century for paper products, bioplastics, gun cotton, and in the construction of the majority of residential structures of North America. Numerous composite materials have been created over the years to more efficiently utilize this resource in the forms of particleboard, plywood, and oriented strandboard. Over the years, structural adhesives for wood composites have moved away from animal and protein based adhesives to synthetic adhesives. Nowadays, the production of adhesive resins for wood composites is a multibillion dollar industry that primarily utilizes phenol formaldehyde and urea formaldehyde formulations that are synthesized from non-renewable resources. These two materials account for over a million tons of resin produced annually.[1] Growing health concerns with formaldehyde emissions have caused urea formaldehyde adhesives to become highly regulated.[2] In response to these regulations, soy-based adhesives were developed from renewable materials.[3] However these resin systems still require the use of fossil fuel derived reactants in their formulation to bond biomass substrates.

Woody biomass is composed of a combination of highly organized polysaccharides and polyphenolics within the cell wall.[4] Cohesion within the woody plant stem is developed from a myriad of intermolecular interactions inherent of the biopolymers, along with crosslinking arising from the process of lignification at the end of cell development. These polymer materials will soften through a glass transition[5] and then begin to rapidly degrade when exposed to heat above 240 °C.[6] The main polymeric components show specific degradation profiles as a function of temperature and this is dependent upon heating rate as well as the environment. Because of the polymeric cellular structure, wood tissue is a thermal insulator.[7] A novel method for wood adhesion was developed by exploiting the poor thermal conduction of wood during frictional heating.[8] Two wood substrates vibrating at a frequency of approximately 100 Hz caused partial degradation of the polymeric components at the surface of wood. The thermal degradation of these

[a]*Macromolecules and Interfaces Institute, Virginia Tech, Blacksburg, VA, 24061, USA*
[b]*Joint BioEnergy Institute, Lawrence Berkeley National Laboratory, Emeryville, CA, 94608, USA*
[c]*Department of Sustainable Biomaterials, Virginia Tech, Blacksburg, VA, 24061, USA*
[d]*Biological and Engineering Sciences Center, Sandia National Laboratories, Livermore, CA, 94551, USA*
[e]*Department of Wood Science, The University of British Columbia, Vancouver, BC V6T 1Z4, Canada. E-mail: scott.renneckar@ubc.ca*

† Electronic supplementary information (ESI) available: Additional analysis of the material including ion chromatography of the water soluble material, ^{13}C CP MAS NMR of the surface material, a schematic of common lignin linkages identified in the 2D HSQC NMR, an extraction scheme for material isolation, and SEM of laser modified cellulose. See DOI: 10.1039/c5ra09676f

components was limited to the interface between the two substrates. Vibrational wood welding research reported that interfacial vibration of solid wood caused enough energy for lignin and hemicellulose to mobilize or flow creating fusion of intercellular components for adhesion through an entanglement mechanism.[9]

Another method of transferring localized heat is through the use of laser technology. Laser processing has been adopted in many manufacturing industries such as the automotive[10] and scientific studies indicate its suitability for large area micromachining,[11] cutting medium density fiber panels,[12] and fiber reinforced composite material processing.[13] In the current work, we proceeded with a controlled approach to surface degradation by laser modification resulting in a wood surface layer that could be used as an adhesive. The conditions needed to prepare wood substrates for adhesion using a CO_2 laser, heat, and pressures were determined to create a new paradigm in assembling natural-based composites. Chemical changes due to laser ablation and interactions of degraded lignocellulosic materials to form adhesive bonds were investigated. This study provided a path for the creation of biobased composites with sufficient properties from a single natural resource, in this case sustainably harvested trees, while providing insight into new methods to convert lignocellulosic biomass into new materials.

Results and discussion

Laser modification and bond strength

Laser modification of the wood surfaces was controlled by the severity of the laser treatment based on laser power, spot size, and line separation. These parameters were quantified as a single laser line intensity, which is the numerical value relating diameter of the spot size (d_{spot}), average power (P_a), laser head speed (v_{scan}), pulse duration (τ_D), and repetition rate (ν) to provide the infrared energy density at the surface. The resulting laser treatments, reported in Table 1, dictated the microscale surface roughness of the samples (Fig. 1). Treatment 1 resulted in ablated channels that were approximately 330 μm in width and 50 μm in depth. Treatment 2 created deep channels that were on the order of 500 μm in width and depth and these geometries mimic wood bonding techniques like finger jointing. Treatment 3 ablated 300 μm of surface material away leaving shallow channels of 60 microns spanning a width of 870 μm. This treatment, overall, created the most even surface roughness. The change in surface was evident by the presence of a darkened layer across the surface, which is typically seen in laser cutting and inscribing of wood.

Table 1 Laser treatment parameters that influence surface properties for bonding

Treatment	Spot size (mm)	Laser power (watts)	Laser head speed (m s^{-1})	Line intensity (W mm^{-2})
1	0.35	30	0.25	1164.2
2	0.69	60	0.10	763.0
3	1.75	60	0.17	28.3

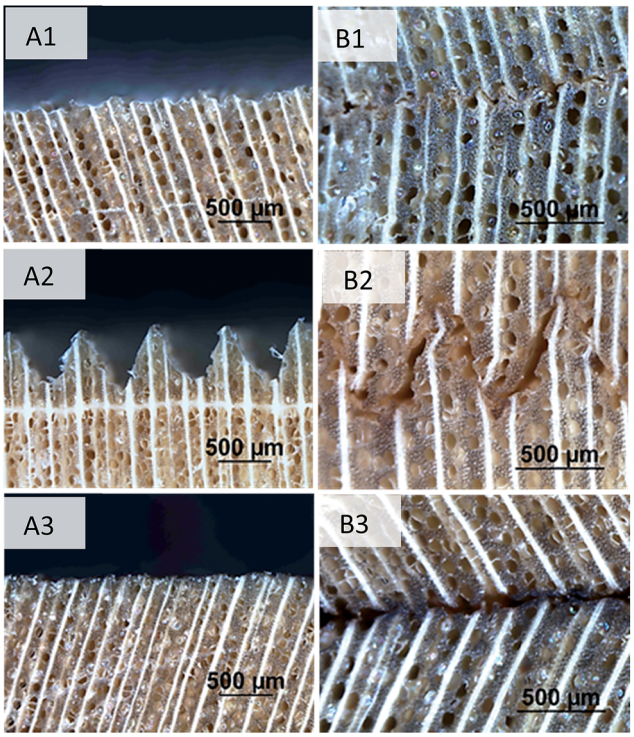

Fig. 1 Cross sectional images of yellow-poplar wood by light reflective microscopy of laser induced surface geometries (A1–3) and subsequent bond lines (B1–3).

Compression shear block testing of the laser modified wood samples bonded together after hot-pressing at 180 °C for 10 minutes showed an adhesive layer performance dependent on laser treatment (ESI Fig. S1†). Stress and displacement curves indicated brittle bond-lines for all laser treatments. Bond-lines with micro-finger joint geometries (Treatment 2) resulted in the lowest average ultimate shear strength amongst the laser treatments at 0.88 MPa (44.5% COV). These specimens delaminated without additional wood failure, which indicated that the adhesive layer is significantly weaker than the surrounding wood. For these samples, microscopy revealed discontinuous and void-filled interfaces suggesting a decrease in contact and frictional interactions between the surfaces. Samples with disjointed surfaces and reduced contact would explain the low test values, as frictional coefficients are often used to estimate the mean shear stress in the adhesive layer.[14] Treatment 1 resulted in bond lines that had intermediate average ultimate strengths of 4.62 MPa (28.4% COV) without additional wood failure. Treatment 3 resulted in the highest average strengths at 6.57 MPa (21.1% COV), which is nearly 80% of the ultimate shear strength of solid yellow poplar.[15] The laser conditions for Treatment 3 were adopted for further analysis, and all subsequent discussions on laser modification refer to this treatment.

CO_2 laser modification of wood and chemical characterization

The initial step to enable self-adhesion of the wood was the laser modification of the surface. Therefore, it was important to observe the laser effect (using 28 W mm^{-2}) on the microscale

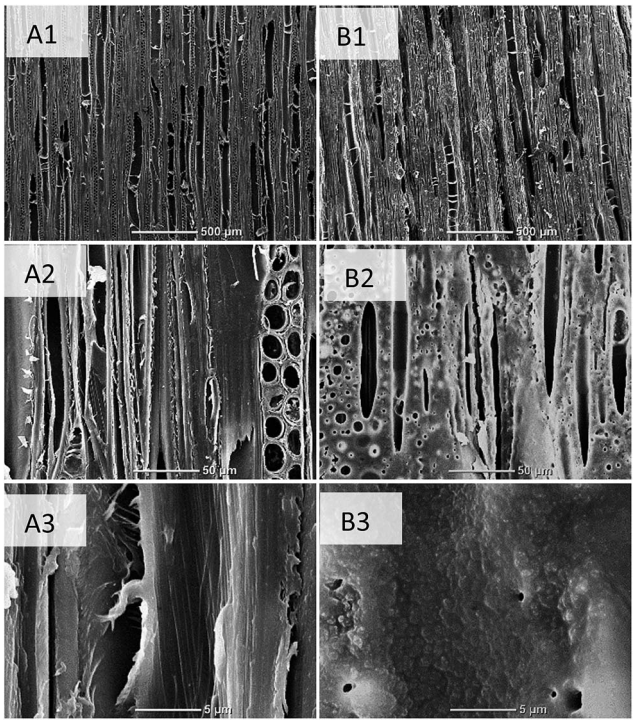

Fig. 2 Scanning electron microscopy images of microtomed yellow-poplar wood (A) and laser modified wood (B) at magnifications of 50× (1), 500× (2), and 5000× (3).

features of wood by (SEM), Fig. 2. The comparison of unmodified and laser modified wood surfaces at 50× showed large wood anatomical features characteristic of this magnification and there were no other significant differences. However, at 500× magnification, there was a clear reduction in cellular features for the laser modified wood. The unmodified wood surface was partially fibrillated from the tearing involved with surface preparation, while the modified surfaces had a cauterized appearance, reducing the protrusions of these wood features. At this magnification some wood anatomical features were identifiable in the laser modified samples, whereas certain cells were fused unlike the control sample. At high magnification, 5000×, vertical microfibril orientation was visible within the control image (Fig. 2). The laser modified wood image showed no such orientation, as the cell wall ultrastructure was absent. The fused cell wall regions provided evidence that the laser energy has the capability to coalesce degraded wood polymeric material by either laser induced thermal flow or from the condensation of volatiles produced from rapid cooling.

Laser modified wood was removed (ESI Fig. S2†) through wet abrasion and chemical changes were analyzed using 2D HSQC NMR, probing ^{1}H and ^{13}C nuclei.[16,17] For the polysaccharide region of the spectra, significant disruption to the xylan is seen for the laser modified wood relative to the control sample (Fig. 3). This degradation is evident by the reduction of the signal for the xylan backbone along with an increased intensity of the reducing ends of the xylan. The former suggests significant degradation, while enhancement of reducing ends results from depolymerisation. The cellulose signal does not have a significant change besides spreading of the signal at ~103 ppm (Fig. 3) from the C_1 carbon and this may relate from the change to the hemicelluloses. Aromatic signals from the lignin polymers contain a few notable changes (Fig. 4). The most significant change to the structure is the reduction in aryl-ether bonds in the lignin (noted as "A" in Fig. 4). The laser modification caused the relative amount of these bonds to be reduced from 71 per C_9 unit to 42 per C_9 unit, revealing that the lignin is partially depolymerized by the laser treatment. Noteworthy was the increase in the number of cinnamyl alcohol end groups

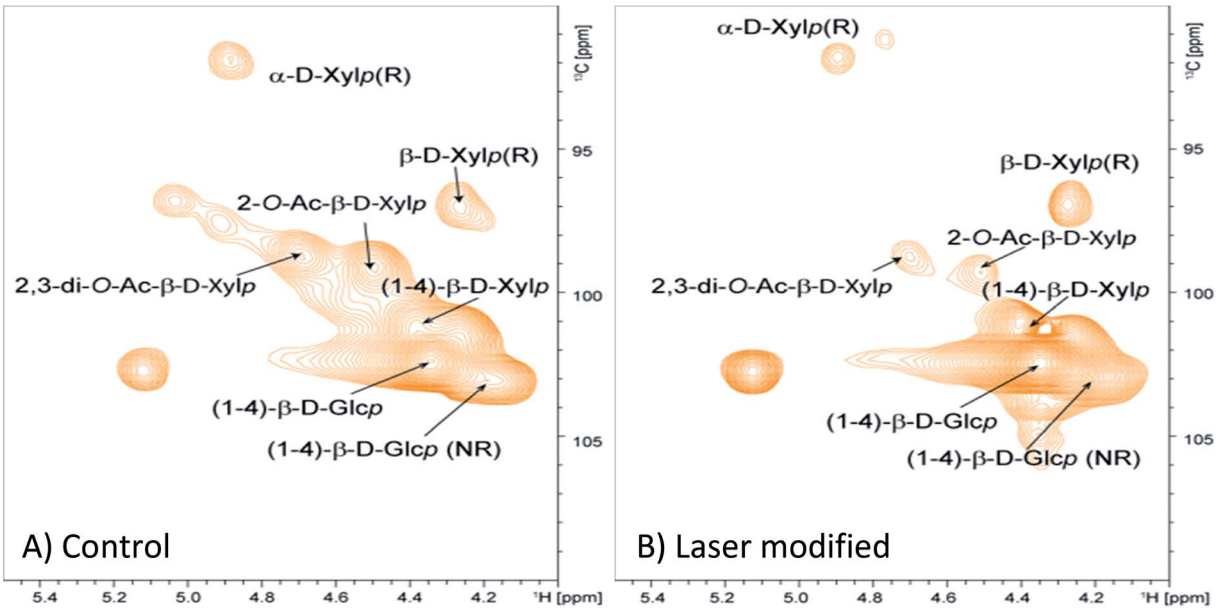

Fig. 3 HSQC NMR spectra of a control specimen (A) and laser modified wood (B) in DMSO-d_6 illustrating significant changes to the polysaccharide region of the wood.

(noted as "E") resulting from the laser treatment (Fig. 4). The relative content of these units double in size, which results from homolytic cleavage of β-O-4 interunit linkages which is found throughout the thermolysis literature.[18] The structural units of lignin change as noted with a decrease in syringyl (S) to guaiacyl (G) ratio from 5.9 to 4.5 (Fig. 4). This decrease in S/G ratio may arise from the loss of methoxy units directly from the ring or a decrease in the S units during depolymerisation and subsequent solubilisation during isolation. It should be noted that syringaldehyde compounds were detected in the water soluble extract from the surface using reversed phase liquid chromatography (see below), which is a potential by-product of the thermal degradation pathway. Additional observations note limited modification of the lignin as the S to oxidized S′ remains at a very high ratio, and the number of the other linkages β-5 and β–β remain without significant change. Overall, laser modification caused limited depolymerisation of the lignin resulting in the creation of more vinyl end groups with minimal oxidization and a slight loss of S units.

The isolated solids portion of the laser modified material was hydrolyzed to determine the relative amounts of structural polymers in the laser degraded surface layer compared to unmodified yellow-poplar. Analysis of the hydrolysate revealed that the laser modified surface layer had increased D-glucan from cellulose and a very small percentage, less than 5 wt%, of xylan, mannan, arabinan, and galactan remaining from hemicellulose relative to the control (Table 2). Out of the four hemicelluloses, glucuronoxylan was the major hardwood

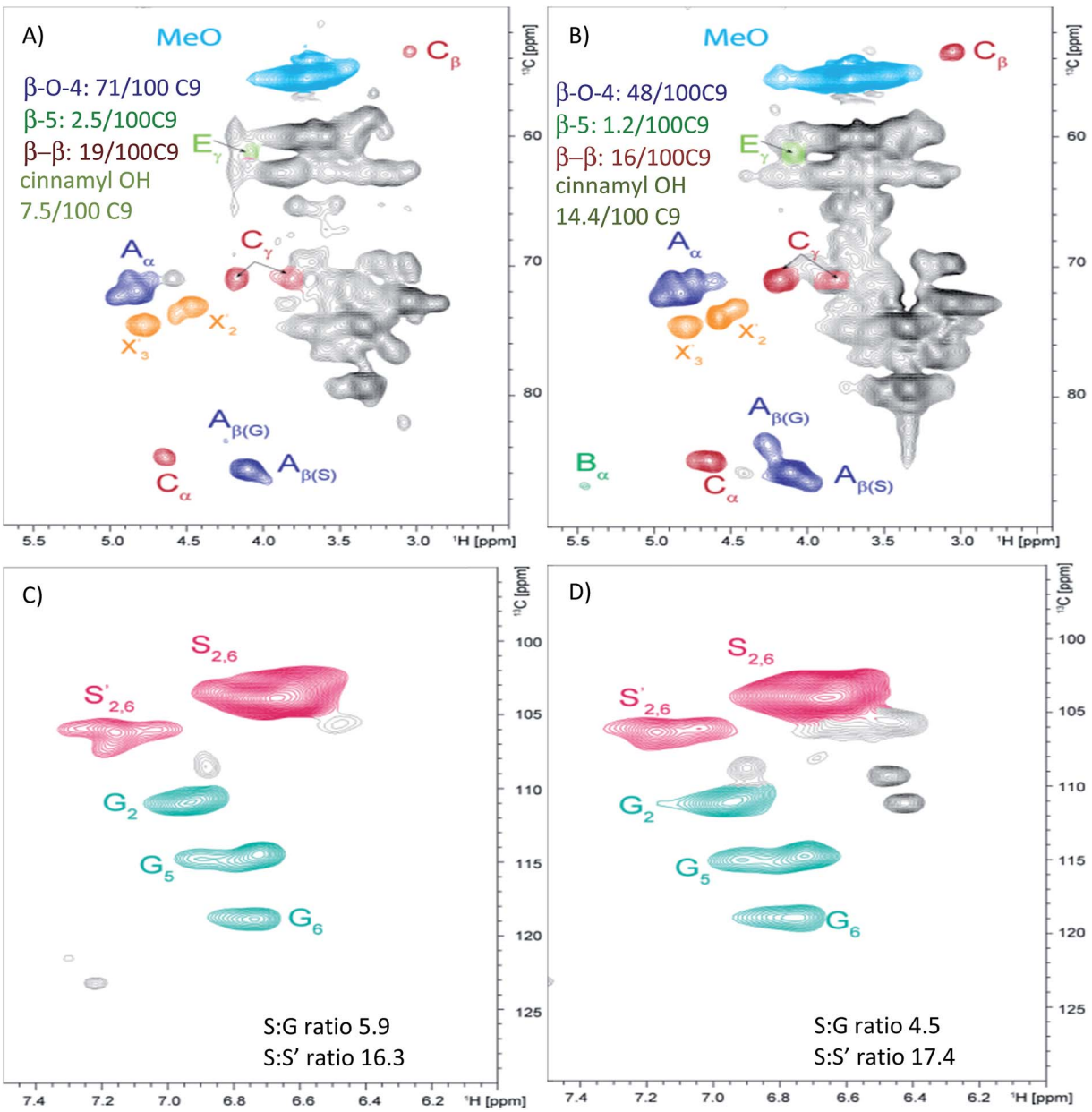

Fig. 4 HSQC NMR spectra of yellow-poplar (A and C) and extracted laser modified wood (B and D) in DMSO-d_6 illustrating differences to the lignin. Color coding relates to specific lignin linkages found in the ESI Fig. S3.†

Table 2 Structural polymer composition of yellow-poplar samples

Sample	Glucose (%)	Xylose (%)	Arabinose (%)	Galactose (%)	Mannose (%)	Acid insoluble lignin (%)	Ash (%)
Control	49.2	13.5	0.36	0.81	0.85	21.09	0.30
Laser modified	63.2	3.8	0.23	0.20	0.36	27.93	0.70
Change	14.05	−9.64	−0.14	−0.61	−0.49	6.84	0.40

hemicellulose comprised of a β-D-xylose backbone. This polysaccharide was significantly affected by laser modification as seen by the significant decrease in D-xylose concentration and also supported in the 2D NMR analysis. Acid insoluble lignin increased due to laser modification, but was only 28% of the total surface layer indicating the majority of the surface, 90%, was composed of cellulose and lignin.

The direct analysis of the water soluble portion of the extracted laser modified wood surface revealed degraded, dehydrated, and hydrogenated products not found in the control wood specimens. The detected compounds include the monomers D-glucose, D-xylose, L-arabinose, sorbitol, xylitol, and levoglucosan (ESI Fig. S4†). These compounds are the result of laser modification leading to the breakdown of major structural wood polymers. The most abundant monosaccharide was D-xylose resulting from the depolymerization of xylan. In lesser extents, levoglucosan and arabinose were also present indicating a thermal degradation product of glucose and another hemicellulose monosaccharide arising from depolymerization. Taken together, rapid heating of the wood surface by laser modification radically impacted the heteropolysaccharides and lead to an enrichment of the surface layer with cellulose and lignin, which is partially depolymerized. The water soluble portion of the surface was estimated to be less than 5% by weight as careful mass balance of the water solubles did not provide repeatable data.

Morphology of the surface layer

The surface of the wood contained areas that appeared as they have flowed together (Fig. 2). To investigate a potential change of the morphology of this layer, isolated surface material was analyzed using X-ray powder diffraction. Surprisingly, the crystallinity index was 84% for both laser modified and control wood using a peak integration method.[19] While native cellulose Iβ peaks in wood were detected that had the four crystalline reflections corresponding to the alignment of cellulose molecules in a lattice including 2θ peaks of 14.5°, 16°, 20.5°, 22° and 34.5°, cellulose II morphology was found in laser modified wood (Fig. 5). Additional peaks for this morphology were noted at 12° and 15.25° along with peaks at 20°, 22°, and 34.5°. Laser modification gave rise to cellulose II structures in laser modified wood, along with the native crystalline peak assignments. Hemicelluloses are known to coat cellulose microfibril bundles and the loss of these components would allow for the crystallization of adjacent fibrils. CP/MAS ^{13}C NMR analysis of the laser modified wood separated by abrasion, supported these changes in crystalline morphology as seen in a resonance shift of the primary hydroxyl groups towards an altered conformation (ESI Fig. S5†). Additional investigation of laser modification of a highly pure cellulose sample showed laser modification can cause significant sintering of cellulose fibrils (ESI Fig. S6†). Cellulose fibrils coalesced and formed a bubble-like topology when exposed to the CO_2 laser energy.

Changes to surface upon heating

In situ heating on an attenuated total reflection (ATR) Fourier transform infrared spectroscopy hot stage was used to detect changes in the functional groups present at the laser modified surface. A 3-D graph of the normalized data, with temperature on the second horizontal axis, was split into hydroxyl and aliphatic signals from 3800 to 2800 cm^{-1} and the fingerprint region from 1800–400 cm^{-1} (Fig. 6). There was a significant change to the hydroxyl stretching region shifting from 3339 to 3442 cm^{-1} and this change grows exponentially above 160 °C. There is also a corresponding relative intensification of the aliphatic stretching at 2900 cm^{-1}. These peak shifts to the hydroxyl region (shift of ~100 cm^{-1}) have been reported to occur during the mercerization process of cellulose[20] including minor shifts (8 to 13 cm^{-1}) at 1230 cm^{-1} and 1030 cm^{-1}, as found in the current spectra (Fig. 6). Additionally, this temperature range of peak shifts was near the onset of a glass transition for laser

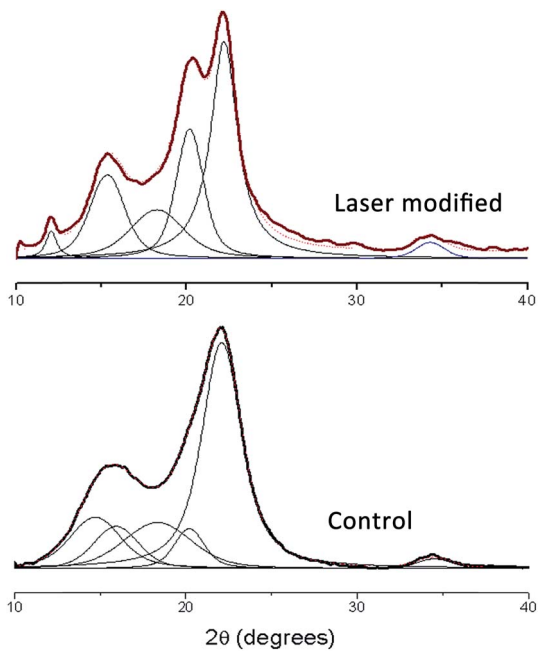

Fig. 5 X-ray diffractograms of yellow-poplar and laser modified yellow-poplar with deconvoluted peaks.

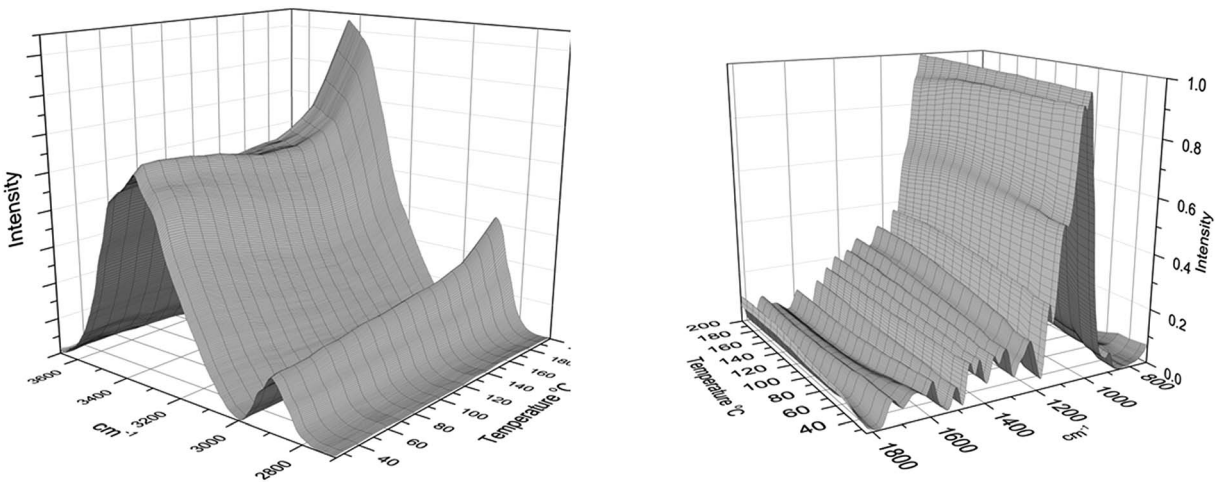

Fig. 6 FTIR analysis of laser modified wood sample analyzed on heated ATR probe stage.

modified wood, as reported in an earlier study,[21] and provides evidence for significant polymer reorganization of the degraded wood components at the surface. A significant change in normalized intensity (over 90%) has been reported during *in situ* FTIR analysis of crystallization of a synthetic isotactic propylene,[22] showing the impact of a morphological change on the spectra. Because of the significant disruption to the cellulose morphology as evidence in Fig. 5, added thermal energy provides additional mobility so components can rearrange into a more thermodynamically stable state. The loss of hemicelluloses along the microfibril surfaces, and breakage of lignin bonds also provides areas for cellulose to shift morphology. Interestingly, laser modified pure cellulose samples failed to show similar trends, which suggests the importance of local mobility and phase separation of the other components impacting the overall morphology of cellulose. Another significant change in intensity happens near 1637 cm^{-1} gradually decreasing from 65 °C to 100 °C, which most likely arises from residual bound water at this temperature boiling off; however, there were no significant changes to the rest of the spectra, such as significant peak shifts or the development of new peaks. The FTIR data revealed that the detectable changes mainly arise from a change in surface

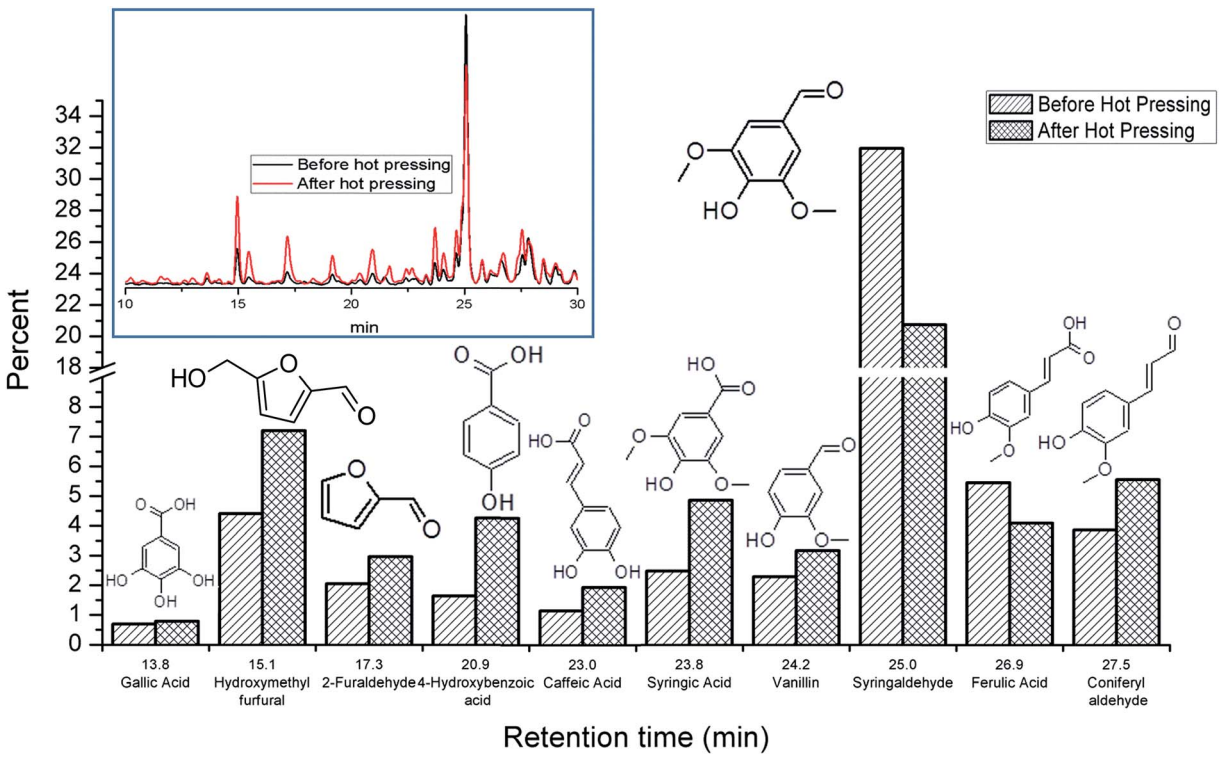

Fig. 7 Percent change in extractable components from before and after hot pressing with retention times and compound structure. Inset: chromatogram of extracted laser modified wood samples.

morphology at high temperatures without significant formation of new chemical groups.

Towards a potential mechanism

The chemical rearrangement and degradation of wood components by laser modification creates an adhesive layer activated by hot pressing. Compounds at the surface for adhesion are stable with time, as additional laboratory tests have shown that adhesion strength is not impacted by the open assembly time between laser modification and hot-pressing from a range of minutes to weeks; this observation indicates that any highly reactive degradation products formed instantaneously after laser modification are not the main compounds involved in adhesion. Additionally, if the samples are heated prior to hot pressing, adhesion capability of the surface disappears in subsequent hot-pressing experiments, revealing the heat activated process is not reversible. Furthermore, for most of the low molecular weight compounds that may cross-link the surface, no significant decrease in concentration were detected before and after hot pressing (Fig. 7). The extracts from the surfaces of the broken samples actually showed a slight increase in most of the degradation products as a result of the hot pressing step, suggesting further modification of lignin and carbohydrates at these press temperatures. The other noteworthy experiment is that post-heating the samples significantly increases the hydrolytic stability of the bond line (ESI Fig. S7†).

Biomass is thermally sensitive at temperatures near the hot pressing condition and recent literature has pointed to the partial degradation of isolated lignin when heated to temperatures above its glass transition temperature.[23] Furthermore, it is reported that aryl ether linkages of lignin with free phenolic substituents reduce the thermal stability of these compounds.[24] After laser ablation of wood, 2-D NMR data shows the loss of β-O-4 bonds and also increased cinnamyl alcohol groups, with the former liberating free phenolics that are less thermally stable and the latter being a possible coupling site on the lignin. Hence, fragmentation of lignin by laser treatment leads to the chemistries that would facilitate free radical mechanisms. These mechanisms can cause condensed lignin structures that lead to a cross-linked polymer. Evidence for this mechanism is seen in increased molecular weight of lignin with thermal treatment[23] along with the thermal stabilization of lignin for carbon fiber precursors.[25] Additionally, Delmotte and coworkers investigated qualitative chemical changes of vibrational welded wood using FTIR and solid state NMR and they found evidence for the removal of methoxy groups of lignin and some degradation to the hemicelluloses.[26] The present study showed substantial loss of all the hemicellulose components because of the laser induced ablation, following similar sensitivity of this component in Delmotte *et al.* study. However, in the current work the 2D NMR spectra show limited change of the methoxy groups through rapid laser heating, so additional crosslinking of the lignin is prohibited at these occupied positions and most likely occurs at the phenolic and propyl chain of the lignin. In support of native chemistries causing bonding, another study reported that heating wood to temperatures beyond the 200 °C (225 to 250 °C) for very long times 60 to 75

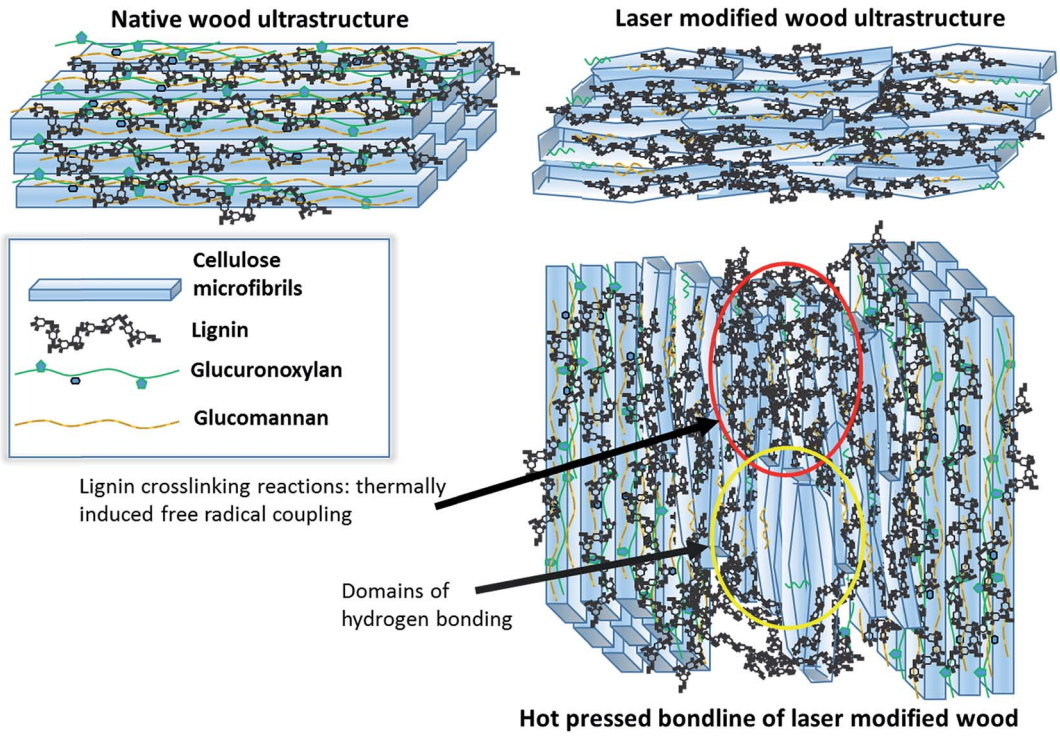

Fig. 8 Illustrative model of laser induced changes of a wood surface at the nanoscale level and hot pressed bondline illustrating potential adhesion mechanism. Note fragmented lignin, reduction in hemicelluloses, and changes in cellulose morphology from laser modification that are found in the modified wood. Because it is a surface sensitive phenomenon wood ultrastructure below the bondline remains unchanged.

min can cause an interphase to develop in unmodified wood veneers; unfortunately, no chemical analysis of the interphase was provided.[27]

Technical lignin has not been commercially developed to serve as an adhesive in its isolated form and this would suggest a limited mechanism of the lignin itself. However, the laser modified surface is only partially lignin with nearly two thirds of the remaining as cellulose. The combination of the mixture of cellulose and lignin with the conditions for radical coupling during hot pressing is the working theory towards adhesion of the samples (Fig. 8). This mechanism is not too unlike the adhesion framework found within the native cell wall, albeit without the same degree of structural order, where intimate interaction amongst the polysaccharides are reinforced by lignin.

Furthermore, the other factor that may add to the adhesion during thermal stabilization is native formaldehyde release from its polymer components. Lignin has been suggested as a source of formaldehyde emission by the elimination of the gamma carbon that results in an ether enol structure.[18] This structure is reported to be hydrolytically unstable and formaldehyde release can cause further crosslinking reactions. *In situ* produced formaldehyde at high temperatures at heat treatment temperatures may be reactive and potentially lead to acetal linkages in the polysaccharides as reported within the cotton textile industry.[28]

Experimental

Materials and laser modification

The solid wood surfaces were compromised of a hardwood, yellow-poplar (*Liriodendron tulipifera*) with dimensions of 3.175 mm thick rotary cut veneers and 0.5 mm maximum Wiley milled wood particles. A Universal V460 60 watt CO_2 pulsed laser, at 10.6 μm wavelength, was used to modify the wood surfaces. The laser's calibrated focal length (5.08 cm), average power (wattage) and carriage speed were varied to increase spot size and influence surface degradation. AutoCAD vector programs were used to control laser carriage movement to accurately separate line ablation based on spot size for complete surface modification. Carriage vectors or laser line direction was parallel to the longitudinal direction of all solid and veneer wood samples.

Compression shear block analysis

A modified ASTM D-905 compression shear block analysis was conducted to determine shear strength of laser modified and hot pressed laminate composites. The laminate and block dimensions were set to 31.25 mm in length, 25.00 mm in width and 9.375 mm in thickness with an offset of 6.25 mm creating 625 mm^2 shear area. Laminates were planed to thickness and conditioned in an environmental chamber at 20 °C at 65.8% humidity (12% wood moisture content (MC)) for two weeks based on the dry weight of wood. Three different laser treatments were used to modify laminate surfaces and were reconditioned to 12% MC prior to bonding. The samples were matched according to grain orientation (*i.e.* tangential surface to tangential surface). Hot pressing conditions consisted of a Micromets Instrument MP2000 Minipress under a constant pressure of 2.0 MPa at 180 °C for 10 min achieving a bond-line temperature above 170 °C. Bonded samples were conditioned at 12% MC and machined to final dimensions and reconditioned to 12% MC until tested.

Light, reflection and scanning electron microscopy

Two specimens of poplar solid wood were cut into approximately 1 cm cubes with a razor blade and soaked in water for 24 h under vacuum. The samples were cut by a microtome to produce two parallel surfaces, one with tangential grain orientation and the other sample with radial grain orientation. Samples were conditioned to 12% (MC) based on the water content related to the dry mass of wood and laser modified on the microtomed surfaces. The cubes were soaked in 95 wt% ethanol for 24 h which limited modified wood and solvent interactions yet provided enough softening for microtoming. A Nikon SMZ1500 reflective microscope was used to capture images of laser induced geometries of poplar shear block specimens.

Two 12% MC 51 × 51 × 3.175 mm (length × width × thickness) poplar veneers were laser modified and pressed with matching longitudinal surface orientation under 2.0 MPa at 180 °C for 5 min. The sample was cut into a 6.5 mm cube and microtomed through the cross-sectional area containing the bond-line. The sample was dried at 103 °C for 24 h and adhered with double sided copper tape to a stage. The sample was sputter coated with approximately 10 nm of gold/palladium (60/40) and analyzed in a NeoScope JCM-5000 JEOL scanning electron microscope operating at 15 kV under high vacuum.

Ion chromatography

Pulse amperometric detection ion chromatography (IC) was used for sugar analysis of the laser modified poplar *versus* remaining bulk wood. Brush extraction with water loosened the thin layer of modified wood from veneers and was collected before and after hot pressing (ESI Fig. S2†). The solid material was isolated with a centrifuge for 30 min at 5000 rpm then decanted. The residue was freeze dried at −40 °C and 40 mTorr for one week. The supernatant was analyzed with IC for laser hydrolyzed and dehydrated monosaccharides. The dried precipitant and oven dried bulk poplar veneer were Wiley milled to obtain 0.5 mm maximum particles and acid hydrolyzed as described elsewhere.[29] Modification to this procedure consisted of analyzing non-neutralized filtered carbohydrate supernatant due to the broad pH tolerance of the IC column. IC parameters consisted of a Metrohm auto-sampler and pump system with ultrafiltration, Hamilton RCX-30 250 mm column, deionized water eluent, 1 mL min^{-1} flow rate, post column reaction (PCR) reagent was 350 mM NaOH, 32 °C column temperature, 1 h determination time, 200 μL injection volume, and Dosino partial loop dilution of samples and standards for calibration. Aqueous sugar standards for calibration included D-arabinose (Sigma-Aldrich), D-galactose (Sigma-Aldrich), and D-mannose

(Sigma-Aldrich) at 100 ppm and D-glucose (Sigma-Aldrich) and D-xylose (Sigma-Aldrich) at 1000 ppm with six separate dilutions of 40×, 20×, 10×, and 4×. Hydrolyzed samples were diluted 40× and laser modified supernatant was not diluted. Water soluble compounds in supernatant were determined through an additional series of sugar standards including D-sorbitol (Sigma-Aldrich), D-xylitol (Sigma-Aldrich), and levoglucosan (Sigma-Aldrich). The standards and supernatant were compared with retention times for molecule determination.

High pressure liquid chromatography

The water soluble phenolic compounds were tested with high pressure liquid chromatography (HPLC) for identification using retention times. The high performance liquid chromatography (HPLC) system included Shimadzu LC-10ADVP pumps, SIL-10ADVP auto injector, SPD-10AVVP UV/Vis detector, SCL-10A VP system controller, CTO-10AS VP column oven and LC solutions software. A Nucleosil 100-5C18 (25 cm by 4.6 mm) column was used at 70 °C with a total flow rate of 0.7 mL min^{-1}. The gradient eluent consisted of 0.025 MKH_2PO_4 buffer with a pH of 2.24 (A) and methanol (B) where the concentration of B increased from 0–50% over 20 min and then increased from 50–70% over the next 10 min. Acquisition time was 30 min, 15 μL injection volume, and UV/Vis detector calibrated to 280 nm. Standards composed of 4 mg mL^{-1} in methanol were used including gallic acid (Sigma), *trans*-ferulic acid (Aldrich), syringaldehyde (Aldrich), syringic acid (Sigma), 4-hydroxybenzoic acid (Aldrich), 4-hydroxy-3-methoxycinnamaldehyde (coniferaldehyde) (Aldrich), caffeic acid (Sigma), vanillin (Sigma-Aldrich), 5-hydroxymethyl furfural (HMF) (SAFC), and furfural (Sigma-Aldrich). Decanted laser modified material was filtered to 0.2 μm and tested.

X-ray diffraction

Samples were prepared from water extracted laser modified material and knifed milled poplar. X-ray diffraction (XRD) was performed using a Bruker D8 Discover XRD system, Cu Kα (λ = 0.154 nm) radiation operating at 40 kV/40 mA. Diffraction profile was detected using a locked couple 2θ scan from 10 to 50°. XRD data was baseline subtracted using Origin Pro 8 and noise reduction was conducted using spectral data averaging. Peak fitting was used to deconvolute peaks for crystallinity index and fit to $r^2 > 0.99$ and $F > 10\,000$. Baseline subtraction and normalization of the spectra along with Voigt area function deconvolution and amorphous halo addition allowed for the integration of all the peaks. Total crystallinity was found though eqn (1).[19]

$$\text{crystallinity}\% = \frac{\text{area under peaks}}{\text{area under peaks} + \text{amorphous halo}} \times 100 \quad (1)$$

2D ^{13}C–^{1}H heteronuclear single quantum coherence (HSQC) nuclear magnetic resonance (NMR) spectroscopy

The unmodified wood sample was extracted to remove extractives and ball milled as previously described.[17,30] The ball milled samples were dissolved in DMSO-d_6 and sonicated till homogenous in a Branson 2510 table-top cleaner (Branson Ultrasonic Corporation, Danbury, CT). The temperature of the bath was closely monitored and maintained below 55 °C. The homogeneous solutions were transferred to NMR tubes. HSQC spectra were acquired at 25 °C using a Bruker Avance-600 MHz instrument equipped with a 5 mm inverse-gradient $^{1}H/^{13}C$ cryoprobe using a q_hsqcetgp pulse program (ns = 200, ds = 16, number of increments = 256, d_1 = 1.0 s).[31] Chemical shifts were referenced to the central DMSO peak (δ_C/δ_H 39.5/2.5 ppm). Assignment of the HSQC spectra was described elsewhere.[17,32] A semi-quantitative analysis of the volume integrals of the HSQC correlation peaks was performed using Bruker's Topspin 3.1 (Windows) processing software. A Guassian apodization in F_2 (LB = −0.50, GB = 0.001) and squared cosine-bell in F_1 (LB = −0.10, GB = 0.001) were applied prior to 2D Fourier transformation.

Cross-polarization magic-angle spinning (CP/MAS) ^{13}C NMR

The cross-polarization magic-angle spinning (CP/MAS) ^{13}C-NMR spectra of water extracted and isolated knife milled samples were obtained on a Bruker Avance-300 spectrometer operating at the resonance frequencies of 300.12 MHz for ^{1}H, and 75.47 MHz for ^{13}C, using a Bruker 4.0 mm MAS NMR probe spinning at 6 kHz. Collection parameters included an acquisition time of 15 ms, a relaxation delay of 1.7 s with 1024 scans. Post-acquisition corrections were made with MestReNova software including a segmental baseline correction, Savizky–Golay normal smoothing, and spectra normalization using the highest peak.

In situ heated FTIR

Laser modified yellow-poplar and unmodified yellow-poplar wood were compared using a heated ATR accessory (GladiATR, Pike Technologies, single bounce diamond plate) on a Thermo Nicolet 8700 FTIR spectrometer. The ATR accessory has a heated stage that was controlled for a temperature ramp where the laser modified material was pressed onto the diamond probe and heated from room temperature to 200 °C at 10 °C per minute with spectra taken every minute consisting of 32 scans with a resolution of 4 cm^{-1}. The spectra were baseline corrected, normalized to the maximum adsorption peak, and meshed into a 3D graph with an axis for wavenumber (x), temperature (y), and intensity (z). The graphical representation of the data was split into hydroxyl and aliphatic signals from 3800 to 2800 cm^{-1} and the finger print region from 1800–400 cm^{-1}.

Conclusion

Laser modification of wood surfaces at energy densities in the range of 30 W mm^{-2} created a unique wood surface that could undergo bonding by hot pressing. Compression shear tests of laser bonded samples indicated average bond strength that was 80% of the wood strength. Compositional analysis of the material at the surface revealed it was predominately composed of cellulose and lignin that had been partially depolymerized. The structural polymer that was most significantly impacted by the laser treatment was xylan resulting in significant removal of

this material. Analysis of the laser modified surface showed an altered surface morphology that appeared to coalesce and further analysis revealed that it contained cellulose II. A theory of radical induced crosslinking of lignin reinforced by cellulose components is provided providing mechanical strength to the bondline. As cellulose and lignin are two of the most abundant polymers found in the world, the manipulation of them into a structural heat setting resin provides a new potential route for the direct utilization of biomass. Moreover, exploitation of this self-adhesion approach would not only eliminate the need of non-renewable adhesives, but also limit the life cycle impact from drilling to transportation of chemical resins.

Acknowledgements

We greatly acknowledge the USDA NIFA Critical Agricultural Materials program grant number 2010-38202-21749 for funding this research. Additionally, a portion of the work conducted by the Joint BioEnergy Institute was supported by the Office of Science, Office of Biological and Environmental Research, of the U.S. DOE under contract no. DE-AC02-05CH11231.

References

1 J. B. Wilson, *Wood Fiber Sci.*, 2009, **42**, 18.
2 US Formaldehyde Standards for Composite Wood Products Act, Title 6, Section 1660, 2010.
3 Y. Liu and K. Li, *Int. J. Adhes. Adhes.*, 2007, **27**, 59–67.
4 D. Fengel and G. Wegener, *Wood: chemistry, ultrastructure, reactions*, Walter de Gruyter, 1983.
5 S. Chowdhury, J. Fabiyi and C. E. Frazier, *Holzforschung*, 2010, **64**, 747–756.
6 M. G. Grønli, G. Várhegyi and C. Di Blasi, *Ind. Eng. Chem. Res.*, 2002, **41**, 4201–4208.
7 W. Handbook, *General Technical Report FPL-GTR-113*, 1999, vol. 24.
8 B. Gfeller, M. Zanetti, M. Properzi, A. Pizzi, F. Pichelin, M. Lehmann and L. Delmotte, *J. Adhes. Sci. Technol.*, 2003, **17**, 1573–1589.
9 B. Gfeller, M. Properzi, M. Zanetti, A. Pizzi, F. Pichelin, M. Lehmann and L. Delmotte, *J. Appl. Polym. Sci.*, 2004, **92**, 243–251.
10 D. M. Roessler, in *High Power Lasers–Science and Engineering*, ed. R. Kossowsky, M. Jelinek and R. Walter, Springer, Netherlands, 1996, vol. 7, ch. 31, pp. 463–504.
11 M. Henry, P. M. Harrison and J. Wendland, *J. Laser Micro/Nanoeng.*, 2007, **2**, 49–56.
12 H. A. Eltawahni, A. G. Olabi and K. Y. Benyounis, *Opt. Laser Technol.*, 2011, **43**, 648–659.
13 C. Brecher, M. Emonts, R. L. Schares and J. Stimpfl, *Proc. SPIE*, 2013, **8603**, 86030H/86031–86030H/86011.
14 E. Serrano, *Int. J. Adhes. Adhes.*, 2004, **24**, 23–35.
15 United States Department of Agriculture and U. S. D. o. Agriculture, *The Encyclopedia of Wood*, Skyhorse Pub., 2007.
16 N. Sathitsuksanoh, K. M. Holtman, D. J. Yelle, T. Morgan, V. Stavila, J. Pelton, H. Blanch, B. A. Simmons and A. George, *Green Chem.*, 2014, **16**, 1236–1247.
17 H. Kim and J. Ralph, *Org. Biomol. Chem.*, 2010, **8**, 576–591.
18 H. Kawamoto, S. Horigoshi and S. Saka, *J. Wood Sci.*, 2007, **53**, 168–174.
19 N. Terinte, R. Ibbett and K. C. Schuster, *Lenzinger Ber.*, 2011, 118–131.
20 S. Y. Oh, D. I. Yoo, Y. Shin, H. C. Kim, H. Y. Kim, Y. S. Chung, W. H. Park and J. H. Youk, *Carbohydr. Res.*, 2005, **340**, 2376–2391.
21 Z. Lin, J. Dolan, C. E. Frazier and S. Renneckar, *Proceedings from the Adhesion Society*, 2013, pp. 181–183.
22 Y. Duan, J. Zhang, D. Shen and S. Yan, *Macromolecules*, 2003, **36**, 4874–4879.
23 C. Cui, H. Sadeghifar, S. Sen and D. S. Argyropoulos, *BioResources*, 2013, **8**, 864–886.
24 R. Brezny, V. Mihalov and V. Kovacik, *Holzforschung*, 1983, **37**, 199–204.
25 J. L. Braun, K. M. Holtman and J. F. Kadla, *Carbon*, 2005, **43**, 385–394.
26 L. Delmotte, C. Ganne-Chedeville, J. M. Leban, A. Pizzi and F. Pichelin, *Polym. Degrad. Stab.*, 2008, **93**, 406–412.
27 H. R. Mansouri, J. M. Leban and A. Pizzi, *J. Adhes. Sci. Technol.*, 2010, **24**, 1529–1534.
28 J. G. Frick and R. J. Harper, *J. Appl. Polym. Sci.*, 1982, **27**, 983–988.
29 A. Sluiter, B. Hames, R. Ruiz, C. Scarlata, J. Sluiter, D. Templeton and D. Crocker, *Determination of structural carbohydrates and lignin in biomass*, Technical Report NREL/TP-510-42618, Golden, 2011.
30 S. D. Mansfield, H. Kim, F. Lu and J. Ralph, *Nat. Protoc.*, 2012, **7**, 1579–1589.
31 S. Heikkinen, M. M. Toikka, P. T. Karhunen and I. A. Kilpeläinen, *J. Am. Chem. Soc.*, 2003, **125**, 4362–4367.
32 D. J. Yelle, J. Ralph and C. R. Frihart, *Magn. Reson. Chem.*, 2008, **46**, 508–517.

